



Development of Mathematical Relationships for Calculating Material-Dependent Flowability of Green Molding Sand

Dheya Abdulamer and Abdulkader Kadauw

(Submitted October 4, 2018; in revised form April 23, 2019; published online May 17, 2019)

Flowability property has a strong influence on the performance of the molding process of green sand. Flowability is the capability of bentonite-bonded green sand for flowing around a model especially in the critical regions during the sand mold-making process. It is a necessary property for obtaining molds without bridge formation and without loss of the energy consumed in the molding process. The old methods are destructive tests usually carried out for measuring flowability of green sand before an actual molding process. Direct tests during the mold-making process are not implemented yet. The new method developed by Bast (Arch Metall Mater 58(3):946–952, 2013) uses two sensors. These sensors are integrated into the template similar to the template of the Orlov test (Mori and Inui in J Jpn Foundry Soc 44(8):659–666, 1972) for live monitoring of flowability of green sand during molding process. Four mathematical mechanisms have been developed for determining material-dependent flowability based on the sensor's signals. Effect of compactability, water content and speed of pressing machine on the flowability of bentonite-bonded green sand has been studied.

Keywords contact area, continuous pressure, green sand mold, material-dependent flowability, stationary old methods

1. Introduction

The green sand mold-making process is the most common metal casting technique, using silica sand as a medium for the mold. The sand is mixed with clay and water and pressed manually or mechanically around the model to be cast. Because of low pattern and materials costs (Ref 1), the mold of green sand is widely used because of the availability of sand, which can be repeatedly used for molding other patterns (Ref 2). The main object in molding is to compact the sand in a manner that faithfully produces the profile of the pattern. This requires sand particle flow using some ramming technique to achieve the necessary object. It has been experimentally determined that up to 40% or more of the compacting force is lost during the squeeze operation due to friction among the flask, sand particles, model and between the sand particles themselves

This article is an invited submission to JMEP selected from presentations at the 73rd World Foundry Congress and has been expanded from the original presentation. 73 WFC was held in Krakow, Poland, September 23–27, 2018, and was organized by the World Foundry Organization and Polish Foundrymen's Association.

Dheya Abdulamer, IMKF, TU - Bergakademie Freiberg, Agricola Str. 1, 09599 Freiberg, Germany; and ERETC, University Of Technology, Baghdad, Iraq; **Abdulkader Kadauw**, IMKF, TU - Bergakademie Freiberg, Agricola Str. 1, 09599 Freiberg, Germany; and Salahddin University Erbil, Erbil, Iraq. Contact e-mail: Dheya.Abdulamer@imkf.tu-freiberg.de.

(Ref 3). The major energy-consuming process during the casting process is the mold making. An undetermined parameter of the mold-making process requires a trial-and-error method to ensure the mold has a high quality. This is time- and energy-consuming and increases the cost of the molding process (Ref 4).

This research depends on the sensor's signals for measuring of material-dependent flowability of the sand mold during the compaction process. The measurements involve calculating the continuous pressure generated in the contact areas between the bottom sensor and the formed sand and between the upper sensor and the formed sand.

2. Former and New Flowability Tests

This preliminary study summarizes the old methods and modern approach for measuring flowability property of the green sand mold.

2.1 Former Methods

The old methods are stationary tests usually accomplished before the compaction process and based on the mold hardness or sand extrusion for measuring flowability property.

Orlov relied on the hardness measurement to determine the flowability of the mold. The base of the sample to be tested has two surfaces. The distance between the bottom surface and the upper surface is 25 mm as shown in (Fig. 1a). The ratio of hardness at the upper surface ($A-FH_1$) to hardness at the bottom surface ($B-FH_2$) is used to obtain flowability percentage (Ref 5).

Levelink (Ref 6) depended on the sand extrusion to measure flowability property of the mold. A bunker is filled with 400 g of sand through funnel and sieve. The bunker has a fast opening

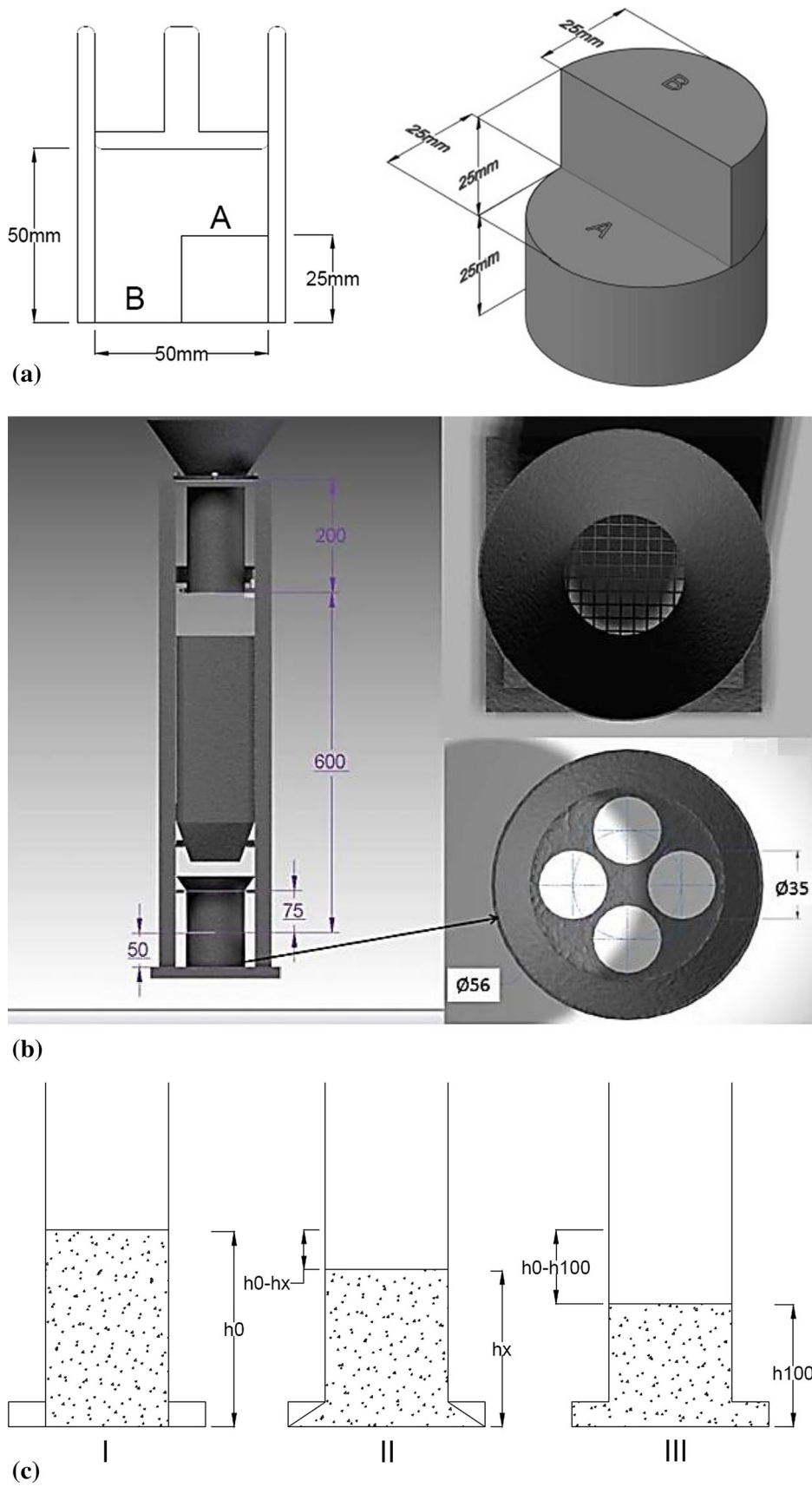


Fig. 1 (a) Flowability method by Orlov (Ref 17); (b) flowability method by Levelink (Ref 8); (c) flowability method by G. Fischer; I: height of AFS specimen, II: height of specimen in test, III: height of ideal specimen (Ref 7)

flap. The space between four extrusion holes and base of the bunker (opening flap) is 600 mm. The sand falls on a sheet through four holes (the hole diameter ϕ is 35 mm) as shown in (Fig. 1b). The relationship between the weight of sand, which is falling through the holes W_h , and the total weight W_t is called the flowability percentage (Ref 6-8).

Fischer used the transverse movement of sand as the criterion of flowability property. He used AFS standard sample height ($h_0 = 50$ mm) to obtain the flowability property. Tools used for inspection include the cylinder test and the discrete base as illustrated in (Fig. 1c). The sand falls toward the cylinder test through the sieve, then rammer the sand through three strikes. The compacted sand fills the discrete base at the end of the cylinder; the ideal sample height h_{100} is 36.3 mm when the groove of discrete base is completely filled. The actual height of the pressed sample (h_x) is calculated, the proportion between $(h_0 - h_x)$ the actual difference of sample height and $(h_0 - h_{100})$ the ideal difference of sample height represents a percentage of flowability (Ref 7, 9).

Kennedy used the same procedure of the Fischer method, but he depended on a ratio of w_x the weight of the sand extruded to w_s the weight of AFS standard sample to determine the flowability percentage (Ref 8).

2.2 A New Flowability Sensor

The spherical sensor has 3 mm radius (R). Both sensors were installed on the upper and bottom levels of the template as displayed in (Fig. 2a). The space between the two sensors is 40 mm. The template has 80 mm diameter, 54 mm height of upper level and 30 mm height of the bottom level, so the difference between the upper and the bottom levels is 24 mm. The dimensions of flowability sensor, cylinder test and piston are shown in (Fig. 2b).

When the piston of the pressing machine is applied on the upper orifice of the cylinder (80 mm diameter), sand movement pushes down a spherical probe of the sensors. The spring which exists under the spherical probe is squeezed so that force changes in the load cell. If the sand does not move the sensor motion is impossible (Ref 10).

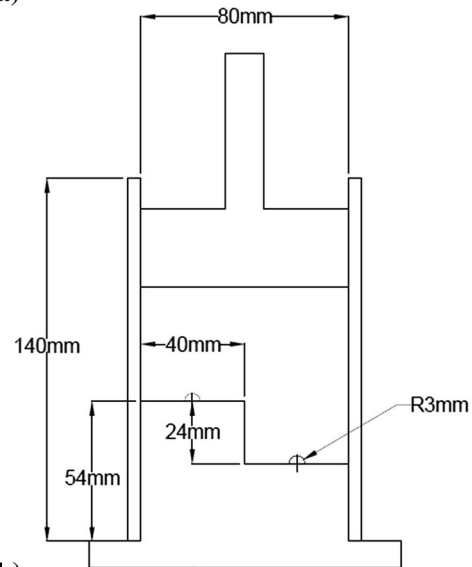
The sensor consists of multi-parts as is shown in (Fig. 3). The load cell 7 is connected with the base 9 at the lower housing 8 and fixed by the screw 10. Compressor part 6 is installed on the load cell. The spacer 4 is installed, and the spring 3 is placed between the compressor part 6 and the sensor probe 1 at the upper housing 2. The latter has connection threads on the inner and outer sides. The upper part is fastened by a nut 5.

3. Investigation of Material-Dependent Flowability

The new method employs sensor's signals for measuring flowability of a sand mold. Parameters of the molding process, which include molding time and air pressure, can be altered using LabVIEW software. The program is set up on a PC for controlling the piston movement. The computer is connected to the pressing machine and flowability sensor for data acquisition from the sensors.



(a)



(b)

Fig. 2 (a) A new flowability sensor; (b) dimensions of tooling used for a new flowability test

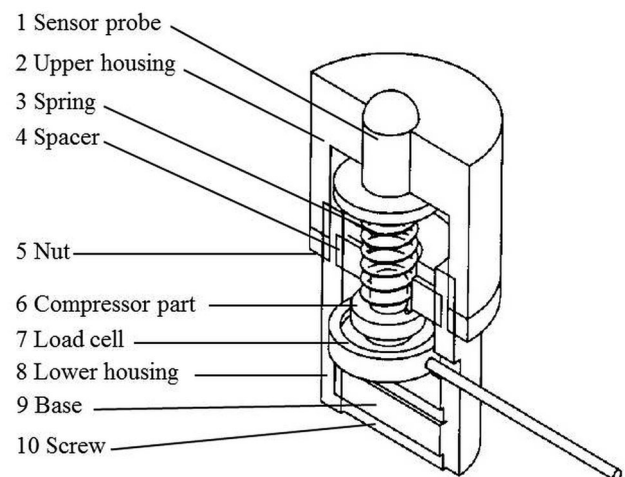


Fig. 3 Components of the sensor structure (Ref 10)

Table 1 Grain size distribution of sand NS

Mesh, mm	0.315	0.2	0.16	0.125	0.1	0.08	0.063	0.063
Residue/sieve, g	0.60	0.8	1.2	2.2	8.6	29.2	26.4	12

Table 2 Characteristics of sand NS₁ and NS₂

Sand type	NS ₁				NS ₂			
	22	27	32	38	48	35	40	45
Compactability, %	22	27	32	38	48	35	40	45
H ₂ O, %	3.46	3.72	3.97	4.58	4.93	4.17	4.67	4.81
Compressive strength, N/cm ²	20.34	15.28	14.89	14.39	17.13	14.88	16.92	17.75
Tensile strength, N/cm ²	2.64	2.99	< 3.3	2.97	< 3.3	1.47	1.66	1.76
Shear strength, N/cm ²	2.73	4.04	4.267	4	4.95	2.91	3.07	3.94

The molding materials used for this investigation are natural sand (NS) and bentonite. Distribution of grain size of natural sand is listed in Table 1. The sand was mixed with 8 and 10% of bentonite to prepare two types of sand NS₁ and NS₂, respectively. Properties of these two types of sand are shown in Table 2. A mixing machine which has a maximum capacity of 6 kg has been used, and the mixing process involves adding 4500 g into the container of the mixing machine. The mixing machine has two steps. The first step is 30 s, and the second step is 3 min; the addition of water occurs during the second step.

The mixed green sand was used to measure the compactability percentage. The tube test (50 mm diameter and 100 mm height) is filled with the sand; then, it subjected into 1 Mpa pressure. Afterward, measurement of loss in the sand, the reduced length of the sand sample represents a compactability percentage.

If the value of compactability percentage does not meet the requirements, thereby adjusting the amount of water, repeating the mixing process and measuring compactability percentage until it obtained the desired compactability percentage (22, 27, 32, 38, and 48%), respectively.

The sand obtained from the mixing machine is saved in a plastic container to protect it from evaporation. Flowability experiments were performed by applying 0.4 MPa pressure through a pressing machine. The molding process was regulated by using 10 s of compaction time and 6 bar of air pressure. The sensor, cylinder, funnel and sieve are placed in the sieve holder, respectively. The cylinder is filled with sand NS₁ through a 5-mm sieve and a funnel to avoid sand aggregation. Sensor and cylinder are placed together in the pressing machine. During the compaction process shown in Fig. 4(a), the signals obtained from the sensors are recorded on the PC as the (S_u) red curve, displacement of the lower sensor and the (S_o) green curve, displacement of the upper sensor as shown in Fig. 4(b), where ΔS is the difference between S_o and S_u .

From the other hand, an influence of the water content and speed of pressing machine on the flowability of sand NS₂ has been also investigated. Pressing speed is (17, 28, and 36 mm/s), and it achieved by adjusting an air pressure (3, 4.5 and 6 bar), respectively.

Amount of water in the green sand has been measured by using the OHAUS MB45 evaporation device, Switzerland. The

test includes placed of maximum 45 g of the sieved green sand into the device. The water will evaporate from the sand, and the water content percentage appears on the screen of the device.

3.1 Mathematical Relationships for Measuring Material-Dependent Flowability (FB)

Depending on the signals of the flowability sensor, several mathematical approaches were developed to calculate material-dependent flowability. These methods are:

3.1.1 Flowability Calculated Based on the Contact Area.

In this method, flowability measurement depends on the stiffness of the sensor spring to calculate the continuous pressure that is generated at the contact areas between the formed sand, the lower sensor and the upper sensor as is illustrated in (Fig. 5).

It is important to emphasize that although the sensor moves, it represents the actual state of stress of the molding material at the measuring point. Since the movement probe of the sensor spring of 1 mm generates a force of 0.855 N (Ref 10), $F_u(t)$ forces that were generated in the lower sensor during (t) the compaction time can be recalculated through multiplying $S_u(t)$ with the spring stiffness 0.855 N/mm.

The area of contact within the lower sensor $a_u(t)$ can be determined through multiplying 2π with square $r_u(t)$ the radius of the contact area between the formed sand and the lower sensor. Multiplying of the sensor radius (R) with the sin function of $\theta_u(t)$ the angle between the formed sand and the lower sensor is used to calculate the radius of the contact area $r_u(t)$. Figure 6 shows a sketch of the head of the sensor; the angle is determined by using an inverse cosine function of ($S_u(t)/R$). The contact-continuous pressure within the lower sensor $P_u(t)$ can be calculated through Eq 1.

$$P_u(t) = \frac{F_u(t)}{a_u(t)}, \quad (\text{Eq 1})$$

The same procedure above was used to calculate the contact area $a_o(t)$ and the continuous pressure $P_o(t)$ at the upper sensor.

Flowability calculations through Eq 2 depend on the proportion of $P_u(t)$ the contact-continuous pressure that is applied in the formed area within the lower sensor to $P_o(t)$ the contact-continuous pressure that applied in the formed area within the upper sensor.

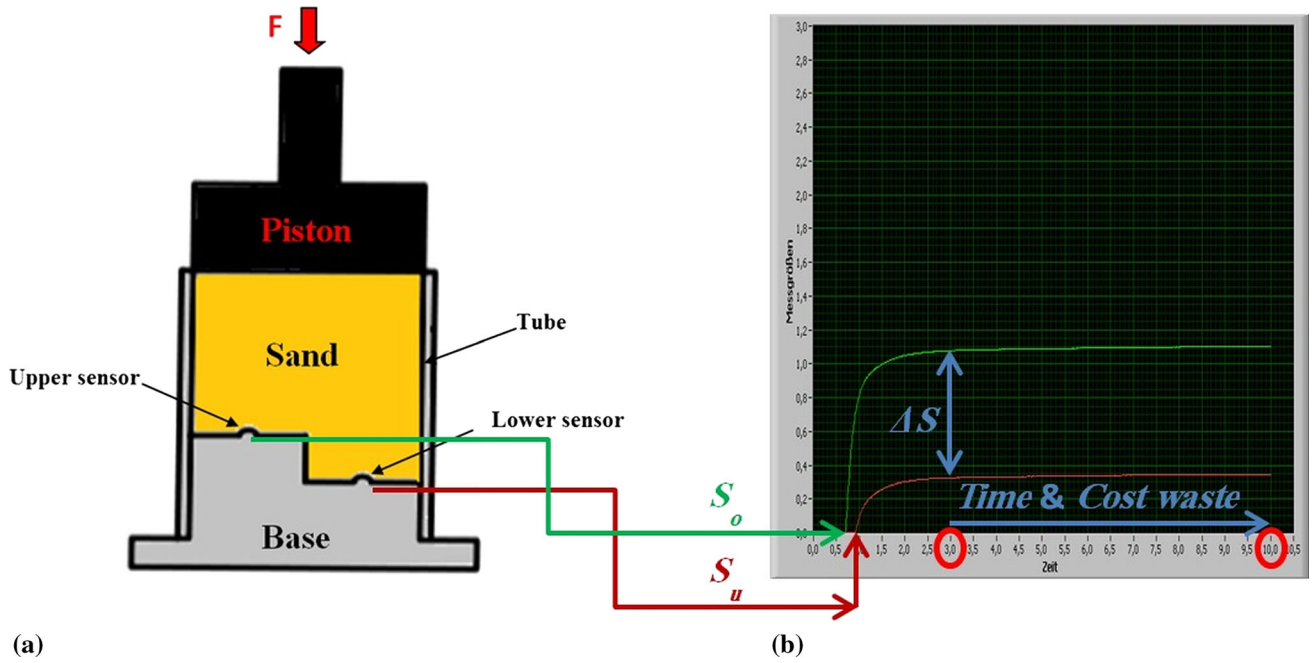


Fig. 4 Compaction process of green sand, (a) principle of the flowability test; (b) sensor's signals

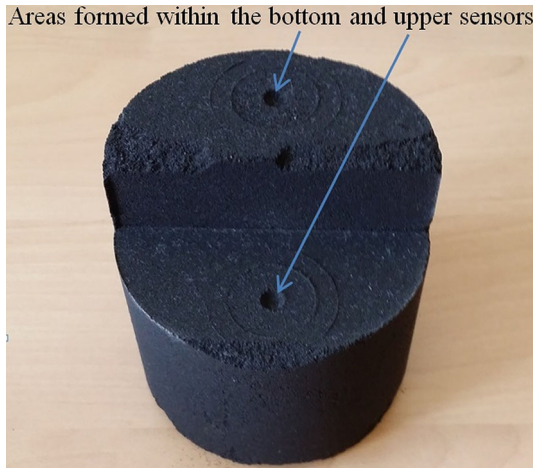


Fig. 5 Flowability sample

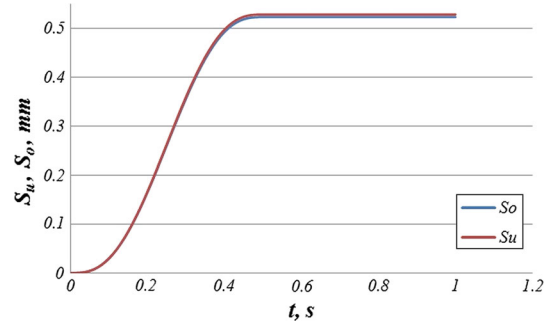


Fig. 7 The ideal situation for the full flow of sand

$$FB(t) = \frac{S_u(t)}{S_o(t)} \times \left[\frac{\sin(\cos^{-1}(\frac{S_o(t)}{r}))}{\sin(\cos^{-1}(\frac{S_u(t)}{r}))} \right]^2 \times 100, \quad (\text{Eq } 2)$$

3.1.2 Flowability calculated based on the distance-dependent pressure. The following formula can be used to express flowability property:

$$FB(\text{mm}) = S_u(\text{mm}) + \frac{S_u(\text{mm})}{S_o(\text{mm})}, \quad (\text{Eq } 3)$$

This relationship indicates that a useful measure of sand flow can be defined by considering two premises:

1. value at the lower level must be high,
2. the ratio of the bottom signal to the upper signal should be 1 (Ref 5). These two factors are shown in Fig. 7; Equation 3 can be rewritten by adding continuous pressure (P_o , P_u) instead of data of the upper and the lower sensor (S_o , S_u).

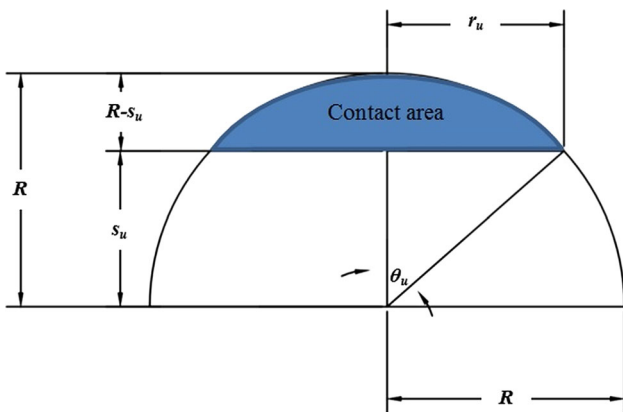


Fig. 6 Sketch of the sensor head

$$FB(\text{MPa}) = P_u(\text{MPa}) + \frac{P_u}{P_o}, \quad (\text{Eq 4})$$

The contact area (a_u) during a 1 mm pushed down of the probe sensor is equal to (50.2655 mm^2). This conversion factor can be used in Eq 5, which can then be used to evaluate flowability values as unitless as well as a percentage.

$$FB(t) = \left(P_u(t) \left(\frac{\text{N}}{\text{m}^2} \times 10^6 \right) \times \left(\frac{50.2655 \times 10^{-6} \text{ m}^2}{0.855 \text{ N}} \right) + \frac{P_u(t)}{P_o(t)} \right) \times 100, \quad (\text{Eq 5})$$

3.1.3 Flowability calculated based on the definite integration. This approach depends on a redrawing of the measured sensor data, finding polynomial equations of the upper and the bottom curves. Afterward, determination of definite integration of A_{o1} the area under the upper curve, and A_{u1} the area under the bottom curve for period time 0-0.01 s. Flowability of the green sand within this period time is expressed through Eq 6. These calculations have been repeated for period time 0.01-0.02 s, and so on until t_{end} time of end signal.

$$FB(t) = \frac{A_{u1}(t)}{A_{o1}(t)} \times 100, \quad (\text{Eq 6})$$

3.1.4 Flowability Calculated Based on the tanh Function. All mathematical relationships above were used to calculate multi-values of flowability during the molding process, but this way is used to calculate only the end value of flowability. In this method, flowability property can be determined depending on the gradient of the curves. The mathematical Eq 7 is an expression of the curves of the sensor signals (Ref 5), where S is the sensor signals, m is the slope of a curve, and S_{end} is the end value of the sensor signal.

$$S(t) = \tan h(m \cdot t) \times S_{\text{end}}, \quad (\text{Eq 7})$$

Equation 7 can be rewritten in terms of S_o , where $S_{o \text{ end}}$ is the end value of the upper curve.

$$S_o(t) = \tan h(m_o \cdot t) \times S_{o \text{ end}}, \quad (\text{Eq 8})$$

m_o slope of the upper curve can be calculated using the genfit function through Mathcad software. The area beneath the upper curve A_o can be calculated by the definite integration of Eq 8 for period time from 0 to t_{end} . The same steps were also used to find the area beneath the bottom curve A_u . The percentage of flowability can be measured through Eq 9.

$$FB(t) = \frac{A_u(t)}{A_o(t)} \times 100, \quad (\text{Eq 9})$$

4. Results and Discussion

Flowability property gives a sign of ability of the sand for flowing during the compaction process without bridge formation. Flowability tests are necessary for ensuring that the mold has uniform properties, especially in the critical regions. The signals obtained from the upper and lower sensors are shown in (Fig. 8). The sensor's signals show an acceleration, constant speed, then slowing down and attain constant value. As the sensor movement depends on the sand movement, this behavior is related to the frictional forces between sand particles, which

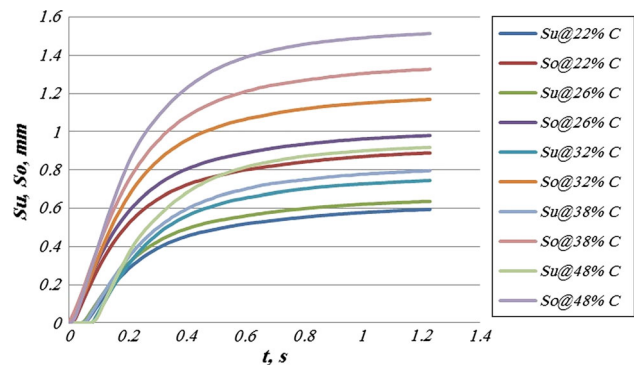


Fig. 8 Signals of the upper and bottom sensors

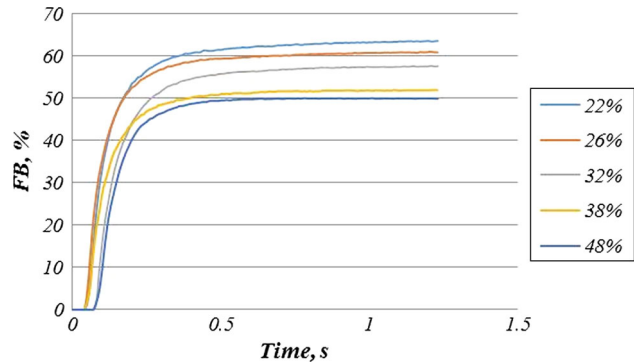


Fig. 9 Curves of flowability obtained through Eq 2

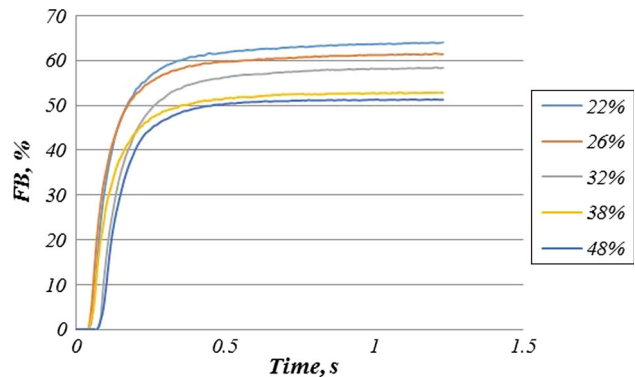


Fig. 10 Curves of flowability obtained through Eq 5

conflict with the sand movement by applying pressure. It was found that different compatibility of the bentonite-bonded green sand NS_1 strongly influences the sensor signals.

Results of material-dependent flowability and final values of flowability were calculated using four mathematical relationships based on the sensor signal's are listed in Fig. 9, 10, 11 and 12.

Flowability changes with the compaction time until it attains a constant value. These results emerged because the formed contact areas within the upper sensor and the bottom sensor (a_o and a_u) decreased during the compaction process. This area reaches the smallest value (0.038 mm^2) when the upper sensor and bottom sensor (S_o and S_u) were pushed down by 2.998 mm. In this case, the flowability of bentonite-bonded green sand mold reaches the maximum value of 100%. The

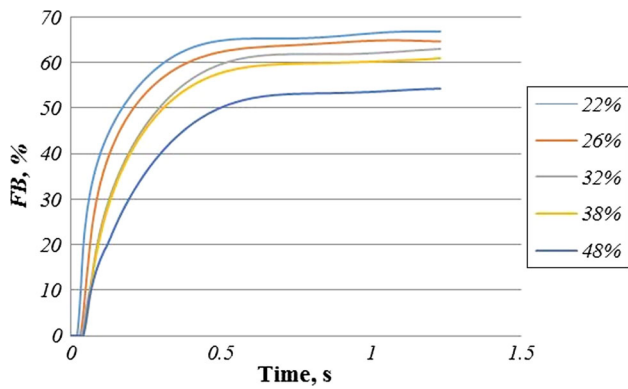


Fig. 11 Curves of flowability obtained through Eq 6

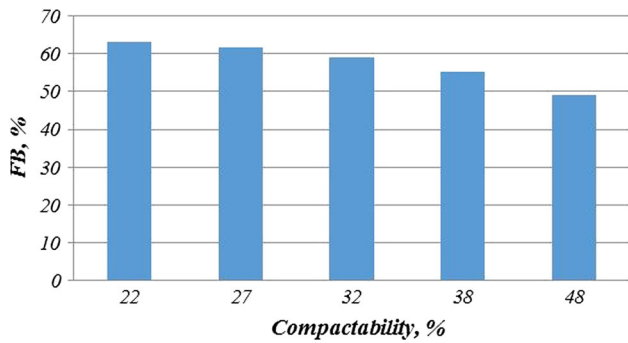
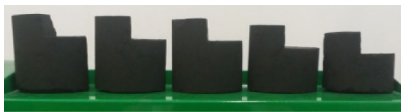


Fig. 12 Bar chart of flowability obtained through Eq 9

Table 3 Final values of S_o , S_u and ΔS

Flowability samples					
Compactability, %	22	26	32	38	48
$(S_u)_{end}$, mm	0.594	0.635	0.744	0.796	0.918
$(S_o)_{end}$, mm	0.888	0.979	1.169	1.328	1.514
$(\Delta S)_{end}$, mm	0.294	0.344	0.425	0.532	0.596

curves of flowability change versus compaction time encourage the foundry men to determine flowability property of the sand mold during the mold-making process, and then to determine valid compaction time, compactability and other parameters of the molding process such as the content of water.

Low flowability existed with the highest compatibility of bentonite-bonded green sand. This problem cannot be solved with increased compaction time because the sand become sticky when the sand has high value of water content or high compactability. Furthermore, the adhesive forces usually developed between molding sand, tube, as well as cohesion force by the binder. These forces have an affect on the flowing of the molding sand in the molding box (Ref 11).

As mentioned in Table 3, mathematically this reason is associated with the high ΔS_{end} difference between the final values of the upper sensor and bottom sensor, while low compactability of bentonite-bonded green sand shows low

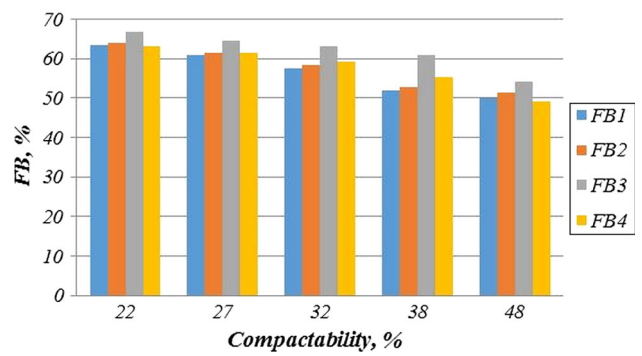


Fig. 13 Bar chart of final flowability obtained through Eq 2, 5, 6 and 9

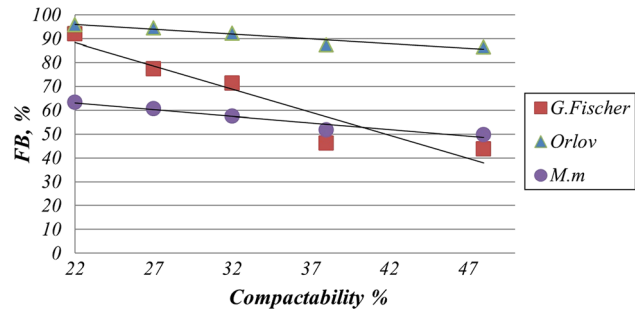


Fig. 14 Effect of compactability on flowability of sand NS1

differences between the final values of the upper sensor and the bottom sensor and so have high flowability percentage. This means that the flowability mainly depends on the compactability of the sand.

Mais et al. (Ref 8) and Tilch et al. (Ref 12, 13) were observed also, that a lower flowability of molding sand occurs with high level of the compactability of molding sand.

In fact, actual behavior of soil is much complicated and shows a great variety of behavior when subjected to different conditions. A few models can describe the sand mold yield. Mohr–Coulomb model is a failure criterion in soil mechanics. The failure of Mohr’s–Coulomb model occurs when the largest Mohr’s circle passing through two principles stresses touches the failure line (Ref 14). The density changes are significant in molding processes. Mohr–Coulomb criterion is not applicable, because this criterion relates only to the individual case of the invariable molding material density. Flow locus can be used to determine real flow limits of molding materials (Ref 15).

Comparisons of end values of flowability obtained through four methods are shown in (Fig. 13). No big differences between flowability obtained by four mathematical functions are seen; therefore, all these mathematical methods may be used for calculating flowability.

Figure 14 and 15 shows a comparison of flowability measured by the Fisher method, Orlov method and Modern method (Mm). The results have shown the same trend; although there is a difference in flowability values their variations are acceptable because the two traditional methods Fisher and Orlov used the standard sample and manual measurements for calculating flowability. This may have an influence on the accuracy of the results. In this context, Khan et al. (Ref 7) and Kadauw et al. (Ref 16) measured flowability by different

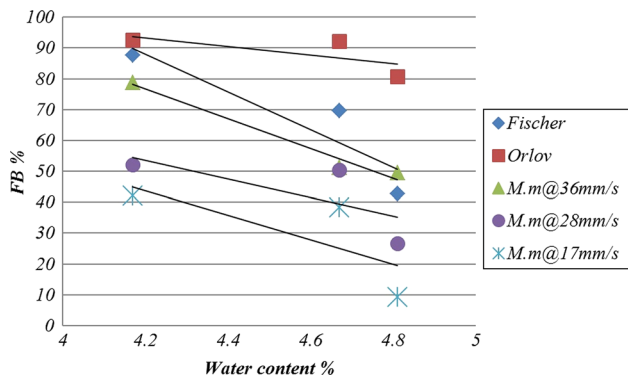


Fig. 15 Effect of water content on flowability of sand NS2

methods. They found differences in flowability values also. Moreover, Fig. 15 shows an effect of water content and speed of pressing machine on flowability obtained by the Modern method. It is found that flowability of green sand NS₂ is inversely proportional to water content and directly proportional to the pressing speed. The smallest value of the speed of pressing machine 17 mm/s gives 42.09, 38.2, and 9.16% of flowability, while 36 mm/s the greatest value of the pressing speed gives 78.82, 51.26, and 49.54% of flowability at 4.17, 4.67, and 4.81% of water content, respectively.

5. Conclusions

The convergence between the final values of flowability allows to use any of the developed mathematical functions for calculating flowability depending on the sensor signals.

According to the conditions of the tests of this research, it is found that 1.23 s of compaction time is sufficient to reach stabilize flowability value. The sand movement depends on the compactability, water content and speed of pressing machine. The sensor movement and subsequent of the signals are based on the sand movement during the compaction process.

Green sand which possesses 22% compatibility shows high flowability percentage, while the sand sample which possesses 48% compatibility shows low flowability. Decreases of water content and increases of pressing speed contribute in improving flowability of green sand.

The final values of flowability calculated by a new approach display good conformity with the flowability obtained by the Orlov method and Fisher method.

Acknowledgments

The author Dheya Abdulamer wants to thank, in particular, the valuable advices, important discussions, encouragement and useful

hints from Prof. Bast, technician Mr. Engmann, Prof. Hentschel, and Prof. Zeidler.

References

1. U.S. Department of Energy, Metal casting, Industry of the future, 2002 annual report. <http://www1.eere.energy.gov/manufacturing/resources/metalcasting/pdfs/annual2002.pdf>. Accessed 08 June 2018
2. C.H. Benson and S. Bradshaw, *User guideline for Foundry Sand in Green Infrastructure Construction*, University of Wisconsin-Madison, Madison, 2011
3. P.D. Webster, *Fundamentals of Foundry Technology*, Portcullis Press Publication, Redhill, 1980, p 404–408
4. J. Bast, A. Kadauw, and A. Malaskin, Optimizing of molding parameters for green sand compaction by computer simulation and a new compaction measuring device, *Int. J. Metal Casting*, 2009, 3(2), p 55–65 (in English)
5. J. Bast, A new method for measurement of flowability of green moulding sand, *Arch. Metall. Mater.*, 2013, 58(3), p 946–952 (in English)
6. H.G. Levelink, H. van den Berg, and E. Frank, Criterion of molding sand quality for modern molding machines, *Foundry Publ.*, 1975, 62, p 1 (in Germanian)
7. R.H. Khan, N.S. Mahadevan, and M.R. Seshadri, *Some Studies on the Flowability of Moulding Sand*, Indian Institute of Science, Bangalore, 1972 (in English)
8. V. Mais, W.L. Guesser, and I. Masiero, Study on the flowability of the Green Sand Molding, *Revista Matéria*, 2014, 19(2), p 94–104 (in Portuguese)
9. F. Hofmann, *Clay-Bonded Moulding Sands*, Foundry Publishing, Düsseldorf, 1975 (in Germanian)
10. A. Malaschkin, *Development of a Method for the Continuous Quality Control of the Green Sand Molding Process with Automatic Molding Machines*, Ph.D. Dissertation, TU-Bergakademie Freiberg, 2002 (in Germanian)
11. A. Kadauw, J. Bast, D. Fiedler, I. Betchvaia, and H.C. Saewert, Computer simulation of squeeze moulding and validation of results using Industrial Computed Tomography (ICT), *Arch. Metall. Mater.*, 2007, 52(3), p 447–451 (in English)
12. E. Flemming and W. Tilch, *Mold Sand Materials and Molding Processes*, German Publisher of basic industry, Leipzig, 1993 (in Germanian)
13. R. Schwarze, J. Bast, W. Tilch, A. Rudert, W. Simon, and H. Belfaqir, *Modeling of Flowing Process of Core Molding Sand as non-Newtonian Fluid Flow*, DFG-Project, TU-Bergakademie Freiberg, Freiberg, 2008 (in Germanian)
14. W.F. Chen and E. Mizuno, *Nonlinear Analysis in Soil Mechanics-Theory and Implementation*, Elsevier, Amsterdam, 1990
15. E. Abdullah, *Investigations between Stresses and Stresses Distribution at Fabrication of Clay-Bounded Molds*, Ph.D Thesis, TU-Bergakademie Freiberg, 2014 (in Germanian)
16. A. Kadauw, *Mathematical Modelling of Compaction Processes of Molding Sand*, Ph.D. Dissertation, TU-Bergakademie Freiberg, 2006 (in Germanian)
17. M. Mori and S. Inui, Green mold characteristics of bentonites and their deterioration on repeated usage, *J. Jpn. Foundrym. Soc.*, 1972, 44(8), p 659–666 (in Japanese)

Publisher's Note Springer Nature remains neutral with regard to jurisdictional claims in published maps and institutional affiliations.